compared to their response during development[2,3,21]. In the CNS, such autocrine loops may exist (1) in motor neurons, which respond to NT-3 during development and also express NT-3 mRNA[23,24]; (2) in substantia nigra neurons which respond to BDNF and express high levels of BDNF mRNA[25,26]; and (3) in hippocampal neurons, which in the adult express high levels of mRNA for all of the neurotrophins[22] and during development respond to BDNF, NT-3 and NT-4/5 (ref. 27). Note that a decrease in BDNF mRNA within the hippocampus has been associated with Alzheimer's disease[28], possibly indicating that a decrease in autocrine function may be a contributing factor to the aetiology of neurodegenerative diseases. □

Received 12 August 1994; accepted 6 February 1995.

1. Lindsay, R. M. *J. Neurosci.* **8,** 2394–2405 (1988).
2. Johnson, E. M. & Yip, H. K. *Nature* **314,** 751–752 (1985).
3. Johnson, E. M., Rich, K. M. & Yip, H. K. *Trends Neurosci.* **9,** 33–37 (1986).
4. Ernfors, P. *et al. Neuron* **5,** 511–526 (1990).
5. Wetmore, C. *et al. Expl Neurol.* **109,** 141–152 (1990).
6. Klein, R. *et al. Cell* **66,** 395–403 (1991).
7. Soppett, D. *et al. Cell* **65,** 895–903 (1991).
8. Squinto, S. P. *et al. Cell* **65,** 885–893 (1991).
9. McMahon, S. B., Armanini, M. P., Ling, L. H. & Phillips, H. S. *Neuron* **12,** 1161–1171 (1994).
10. Becker, D., Meier, C. B. & Herlyn, M. *EMBO J.* **8,** 3685–3691 (1989).
11. Morrison, R. S. *J. biol. Chem.* **266,** 728–734 (1991).
12. Agris, C. H., Blake, K. R., Miller, P. S., Reddy, M. P. & Tsó, P. O. P. *Biochemistry* **25,** 6268–6275 (1986).
13. Zamecnik, P. C. & Stephenson, M. L. *Proc. natn. Acad. Sci. U.S.A.* **75,** 280–284 (1978).
14. Wu-Pong, S., Weiss, T. L. & Hunt, C. A. *Pharmaceut. Res.* **9,** 1010–1017 (1992).
15. Doherty, P., Mann, D. A. & Walsh, F. S. *J. Neurochem.* **49,** 1676–1687 (1987).
16. Ip, N. Y. *et al. Proc. natn. Acad. Sci. U.S.A.* **89,** 3060–3064 (1992).
17. Ip, N. Y. *et al. Neuron* **10,** 137–149 (1993).
18. Acheson, A., Barker, P. A., Alderson, R. F., Miller, F. D. & Murphy, R. A. *Neuron* **7,** 265–275 (1991).
19. Ernfors, P., Lee, K.-F & Jaenisch, R. *Nature* **368,** 147–150 (1994).
20. Jones, K. R., Fariñas, I., Backus, C. & Reichardt, L. F. *Cell* **76,** 889–999 (1994).
21. Lindsay, R. M. in *Sensory Neurons: Diversity, Development and Plasticity* (ed. Scott, S. 404–421 (Oxford Univ. Press, New York, 1992).
22. Kokaia, Z. *et al. Proc. natn. Acad. Sci. U.S.A.* **90,** 6711–6715 (1993).
23. Schechterson, L. C. & Bothwell, M. *Neuron* **9,** 449–463 (1992).
24. Wong, V., Arriaga, R., Ip, N. Y. & Lindsay, R. M. *Eur. J. Neurosci.* **5,** 466–474 (1993).
25. Hyman, C. *et al. Nature* **350,** 230–232 (1991).
26. Gall, C. M. *et al. Molec. cell. Neurosci.* **3,** 56–63 (1992).
27. Ip, N. Y. *et al. J. Neurosci.* **13,** 3394–3405 (1993).
28. Phillips, H. S. *et al. Neuron* **7,** 695–702 (1991).
29. Klein, R., Conway, D., Parada, L. F. & Barbacid, M. *Cell* **61,** 647–656 (1990).
30. Middlemass, D. S., Lindberg, R. A. & Hunter, T. *Molec. cell. Biol.* **11,** 143–153 (1991).

ACKNOWLEDGEMENTS. We thank N. Ip and L. Pan for preparation of RNA and northern blots, and D. Valenzuela and J. Griffiths for synthesis and purification of oligonucleotides.

Dynamic organization of motor control within the olivocerebellar system

John P. Welsh, Eric J. Lang, Izumi Sugihara* & Rodolfo Llinás

Department of Physiology and Neuroscience, New York University Medical Center, 550 First Avenue, New York, New York 10016, USA

WHAT is the role of the cerebellum in motor coordination? Such coordination depends upon the integrity of the inferior olive, a major cerebellar afferent, as its lesion produces ataxic and dysmetric movement abnormalities[1,2]. Using multiple-microelectrode recordings, we report here that there are domains of Purkinje cell activity that are generated by olivary input during skilled tongue movements in rats. Such activity domains are highly rhythmic and time-locked to movement. Patterns of synchronous olivocerebellar activity are geometrically complex and can change during a sequence of movements. The results support the view that the inferior olive organizes movement in time, by entraining motor-neuronal firing through rhythmic activation of the cerebellum, and in space, by synchronously activating cell ensembles that allow the use of individual muscles. Dynamic repatterning of olivocerebellar synchrony may allow different combinations of muscles to be used for movements intended to have varying spatial structures.

Bursts of action potentials known as the complex spike[3] were recorded simultaneously from 26–29 Purkinje cells with as many microelectrodes individually placed into a 1.7–2.8 mm^2 area of cerebellar cortex. Each complex spike is triggered by a single climbing-fibre afferent, which represents the axonal terminal of an inferior olivary neuron[3,4]. Thus, the firing of a single inferior olivary neuron can be inferred from the occurrence of a complex spike in a Purkinje cell[5–7]. Because the Purkinje cell is the sole efferent neuron of the cerebellar cortex, the recordings also reveal the output of this structure. Multiple-microelectrode recordings were obtained from rats trained to protrude their tongue towards a target in front of their mouth. In four such animals, in which long-term recording was stable for over 4 h, olivocerebellar activity during a total of 5,679 movements was analysed.

The behaviour consisted of rhythmic trains of licks having an average duration of 465 ± 25 ms (mean $\pm$ 1 s.e.m. of 3 normal rats; Fig. 1*a*). On average, a train consisted of 4 licks at a mean frequency of 6.7 ± 0.2 licks per s (Fig. 1*a*). The tongue was retracted into the mouth before the mouth closed and another lick was initiated. There were slight temporal differences in the licking of the rats[8]: the licking of rat 2 was the most uniform, as indicated by sharp peaks in the lick autocorrelogram (Fig. 2*b*), whereas rat 3 showed substantial temporal dispersion (Fig. 2*c*), indicating variability in this rat's motor output. For analysis, complex spike data during trains of licks were compared with control periods of equal duration in which there were no licks.

Although previous studies of the olivocerebellar system have generally not indicated a strong relation between single neuron activity and movement[9], the multiple-microelectrode method demonstrates that the olivocerebellar contribution to movement is uniquely coded in the population activity. During a train of licks, multiple Purkinje cell recordings revealed a 270% increase in the incidence of complex spikes due to a doubling of the number of Purkinje cells firing complex spikes (from $24 \pm 6\%$ during a period of rest to $49 \pm 9\%$; $t(2) = 8.9$; $P < 0.05$; Fig. 1*b*) and a 36% increase in the number of complex spikes fired by single Purkinje cells during each licking train (from 1.2 ± 0.03 to 1.6 ± 0.1 spikes; $t(81) = 6.9$; $P < 0.01$; Fig. 1*c*). When Purkinje cells fired complex spikes during a train of licks, the modal number of complex spikes was one; only 24% of the cells fired an average of more than two complex spikes during a train of licks. In fact, the probability that a Purkinje cell fired a complex spike in the 100 ms surrounding a lick was quite low (only $17.7 \pm 2.0\%$ versus $6.5 \pm 0.6\%$ during 100 ms of rest, $n = 82$, $t(81) = 10.7$, $P < 0.01$), confirming findings made during skilled limb movements[9].

Crosscorrelation[10] of the population complex spike activity to the behaviour revealed that olivocerebellar activity was highly rhythmic and significantly related in time to movement ($P < 0.05$), and 74% of the Purkinje cells fired complex spikes in significant temporal relation to the licking ($P < 0.05$). Maximum correlations occurred within 20 ms of the tongue reaching the target, the time of maximal olivocerebellar activity being 1.3 ± 0.9 ms before the lick (Fig. 2).

Spatial analysis of synchronous olivocerebellar activity during movement was derived from zero-time (within 1 ms) crosscorrelation coefficients, a measure of the degree of synchronous firing between cell pairs[11]. A matrix of zero-time crosscorrelation coefficients was generated for every cell in the array (serving as

* Present address: Department of Physiology, Tokyo Medical and Dental University, School of Medicine, 1-5-45 Yushima, Bunkyo-ku, Tokyo 113, Japan.

'master'[5–7]) for periods of movement and for periods of rest. The crosscorrelation coefficients were calculated as follows: the spike train of a cell was represented by $X(i)$, where i represents the time step ($i = 1, 2, \ldots N$ ms) from the beginning of the experimental period; $X(i)$ equalled 1 if the onset of a complex spike occurred at the ith ms, otherwise $X(i)$ equalled 0; $Y(i)$ was the same as $X(i)$, but for the 'master' cell; the crosscorrelation coefficient was represented by $\sum_{i=1}^{N}\{V(i)W(i)\}/\sqrt{\{\sum_{i=1}^{N}V(i)^2\sum_{i=1}^{N}(W(i)^2\}}$ where $V(i)$ and $W(i)$ were normalized forms of $X(i)$ and $Y(i)$, respectively, $V(i) = X(i) - \sum_{i=1}^{N}X(i)/N$ and $W(i) = Y(i) - \sum_{i=1}^{N}Y(i)/N$, to correct for state-dependent changes in firing rate. The mean and variance of each master cell's correlation matrix for the rest period, calculated from the non-zero elements in the electrode array, was used to convert the correlation matrix corresponding to the movement period into standard deviation units, thereby allowing statistically significant ($P < 0.05$) increases in synchrony to be determined[12]. This procedure revealed groups of cells that fired synchronously

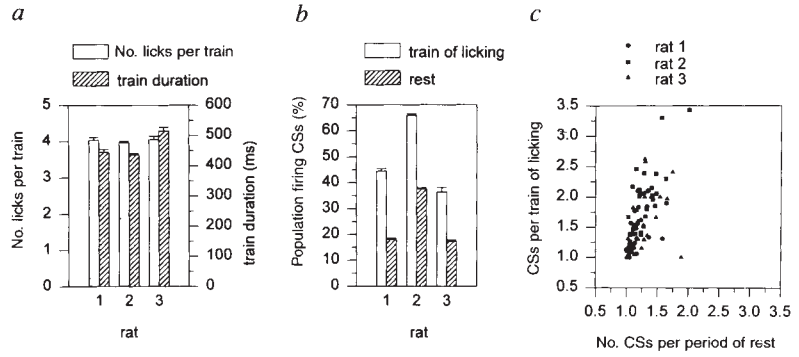

FIG. 1 Population activity within the olivocerebellar system during trains of licking as determined by multiple-microelectrode recordings. A train was defined as 3 or more licks within 600 ms. *a*, The characteristics of the licking behaviour of three normal rats. Trains of licking consisted of 4.0 (±0.02) licks, on average, (white bars) within a mean period of 465 (±25) ms (striped bars). *b*. The mean percentage of Purkinje cells firing one or more complex spikes during a train of licking (white bars) and during an equivalent period of behavioural rest (striped bars) for each of the three rats. A significantly larger percentage ($P < 0.05$) of the Purkinje cell population fires complex spikes (cs) during trains of licking than during rest in each of the rats. For rats 1 to 3, respectively, complex spikes of 26, 29 and 27 Purkinje cells were recorded simultaneously. *c*, The mean number of complex spikes fired by each Purkinje cell during a train of licks and during an equivalent period of rest in the three rats ($n = 82$ Purkinje cells). Time periods in which Purkinje cells did not fire a complex spike were not included in the analysis. Error bars display 1 s.e.m.

METHODS. Four Sprague–Dawley albino rats (200–250 g) were operantly conditioned to extend their tongue towards a metal tube placed 6 mm in front of the mouth to receive a single 40 μl drop of water in a discrete-trial model with a tone (750 ms, 2 kHz, 85 dB) as the conditioned stimulus. After the completion of training, and under ketamine anaesthesia (100 mg per kg, i.p.), the left hemispheral cerebellar cortex was exposed and a silicon-rubber coated titanium grid was placed over the crus IIa folium through which up to 39 glass microelectrodes (saline filled, 1–2 mΩ, 2–4 μm tip diameter) were independently positioned 100–125 μm below 3 mm^2 of the cortical surface. Interelectrode distance was 250 μm. The surrounding margin of the silicon-rubber grid was coated with silver and was used as the ground to prevent contamination of the neural signals with electromyogram artefacts. Extracellularly recorded complex spikes were amplified by a factor of 1,000 and digitized by a single-level threshold discriminator set manually for each channel as previously described[5–7]. Rats recovered from the anaesthesia before a 4-h session of operant conditioning began. Licks were monitored with an infrared photoemitter and photosensor apparatus placed directly underneath the end of the metal tube. Jaw openings and closings were monitored with a second infrared photoemitter and photosensor apparatus positioned under the mandible in its resting position. Lick latency was defined as the time when the tongue interrupted the infrared photobeam. Latencies for mouth opening and closing were defined as the times that the mandibular photobeam was interrupted and restored, respectively. The times of the digital neural and behavioural signals were recorded by a personal computer which scanned all of the inputs within 10 μs at 1 kHz. Only complex spikes from electrodes in which single Purkinje cells were isolated for the entire 4-h duration of the experiment were analysed (~75% of the electrodes). The electrode arrays covered between 26 and 44% of the crus IIa folial surface[25]. The behavioural session during the electrophysiology experiment provided ~500 opportunities to receive water reinforcement. For analysis, control data were taken randomly from a 4-s period beginning 5 s before onset of the conditioned stimulus. There were no mouth movements or licks during the control period. Oral and perioral deafferentation was surgically produced in one rat by bilaterally sectioning the superior labial, mental, and external nasal branches of the trigeminal nerve 12 h before the experiment. The effectiveness of the deafferentation was verified after the experiment by stimulating the face and oral mucosa with a metal probe.

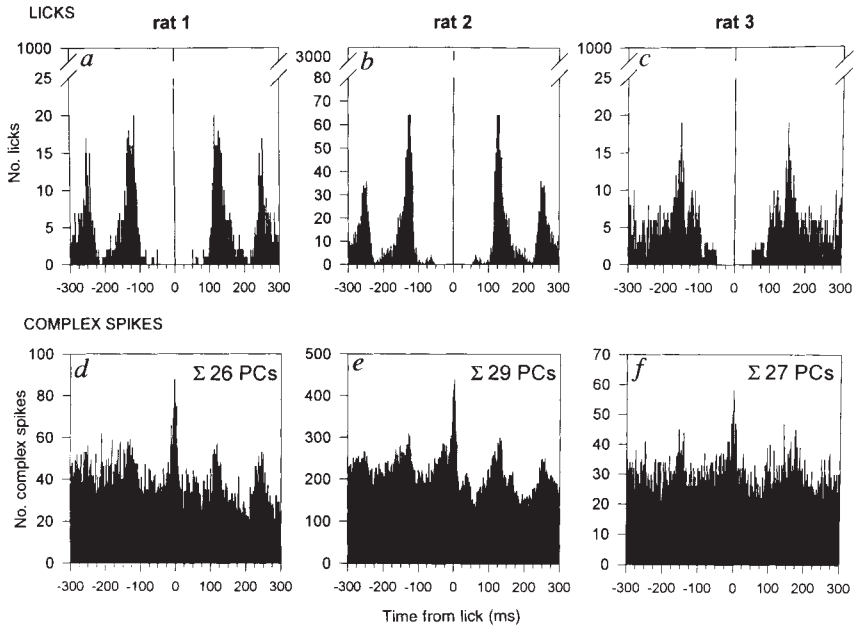

FIG. 2 Complex spike activity among populations of Purkinje cells is rhythmic and temporally related to conditioned rhythmic licking. An autocorrelogram of licking (*a–c*) is presented with a crosscorrelogram of complex spike activity (*d–f*) for 3 normal rats. The tongue movements are highly rhythmic and have a frequency of ~7 Hz. The population complex spike activity from each rat is also highly rhythmic and significantly correlated in time with the licking (all correlation values >0.2 and $P < 0.05$). Times of peak correlated activity are 4 ms before, 1 ms after, and simultaneous with the time of maximal tongue protrusion for rats 1–3, respectively. Bin widths, 1 ms.

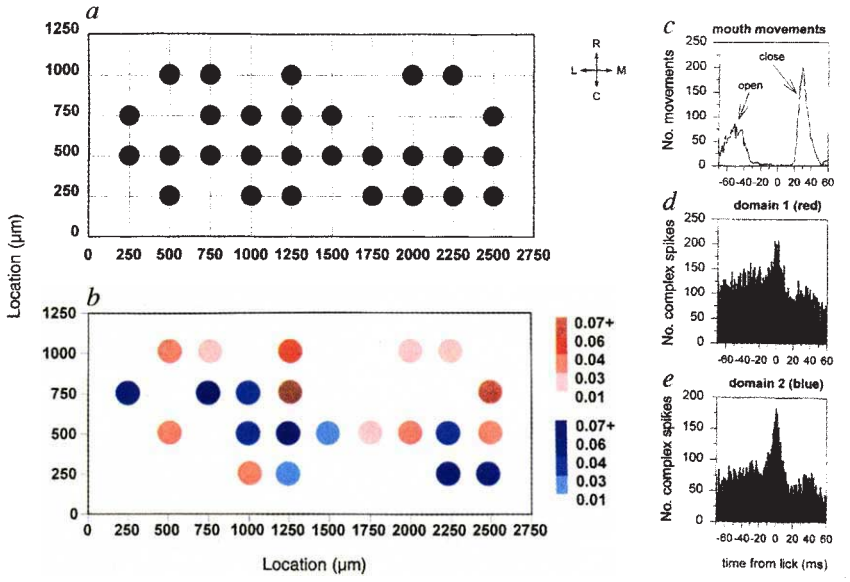

FIG. 3 Spatio-temporal analysis of olivocerebellar activity in rat 2 during rhythmic licking. *a*, The location of 29 electrodes placed within 1.7 mm^2 of the left crus IIa. *b*, The spatial location of two non-overlapping domains of Purkinje cells that fire complex spikes synchronously. *c*, The time of mouth opening and mouth closing in relation to 3,061 licks (time 0). *d*, *e*, The temporal distribution of complex spikes within the red (*d*) and blue (*e*) domains of Purkinje cells relative to the time of maximal tongue protrusion. Note the gradual increase in complex spikes that precedes the sharp peak surrounding the lick and the second peak coincident with mouth closing. Bin widths, 1 ms.

with the master cell of each matrix during movement. Master cells whose groups of synchronously firing cells were at least 70% overlapping were combined and the average degree to which every cell in the array was correlated to members of this assembly was displayed in a plot depicting the surface of the folium. Identical patterns could be obtained when the criterion was reduced to as low as 10%; however, lowering the criterion below 40% introduced additional cell groups whose degree of synchrony was as much as 43% less than the groups obtained by using the more conservative criterion. Thus, the more stringent criterion was adopted to identify the most reliable patterns of synchronous firing, recognizing that less robust patterns could be obtained with more liberal criteria. Purkinje cells that fired synchronously with more than one assembly were represented multiply in the plots, indicating a reorganization of synchronous firing within the inferior olive. Only spatial patterns whose magnitude of synchronous activity during movement exceeded that during the rest period, as determined by analysis of variance ($P<0.05$), are presented.

In one of the three subjects (rat 2), the spatial organization of synchronous firing contained two mutually exclusive domains of Purkinje cells. One domain was non-continuous on the cortical surface and consisted of 4 clusters of cells (red domain, Fig. 3*a*, *b*), whereas the other domain consisted of an obliquely oriented band of Purkinje cells, flanked medially by a small cluster of cells (blue domain, Fig. 3*b*). Although the firing profiles of the groups were similar (Fig. 3*d*, *e*), they did not fire synchronously. Thus, their influences as ensembles must have occurred at different times during individual movements or for different movements.

A dynamic organization of synchronous olivocerebellar activity was found in the other subjects. In these cases, Purkinje cells fired complex spikes synchronously in a variety of combinations during movement. Patterns of synchronous olivocerebellar activity varied as the mouth opened and closed and as the tongue was protracted and retracted (Fig. 4). For example, in the case of the normal rat displayed in Fig. 4*b*, a cluster of 6 Purkinje cells in the postero-medial quadrant of the folium fired synchronously while the mouth opened before the lick. This cluster also fired synchronously when the tongue contacted the target but, at that time, in combination with a rostro-caudal band of 7 Purkinje cells positioned 750 μm laterally. When the tongue was retracted and the mouth began to close, the members of the laterally positioned rostro-caudal band tended to fire synchronously whereas the cluster of cells that fired in relation to opening of the mouth did not fire synchronously.

The spatial organization of synchronous olivocerebellar activity during movement was not produced by the sensory consequences of the movement, as determined in one rat in which sensory branches of the trigeminal nerve innervating the oral and perioral structures were sectioned. Deafferentation disrupted neither the temporal sequence of mouth and tongue movements (Fig. 4*c*) nor the capacity for synchronous firing and the dynamic repatterning of olivocerebellar synchronicity during such movement (Fig. 4*b*).

Our results demonstrate that olivocerebellar control of movement derives from populations of olivary neurons operating as a distributed system whose collective activity is rhythmic and temporally related to specific parameters of movement. Although olivary neurons fire infrequently during sequences of movement, they do so at highly defined moments, indicating that olivary control of movement is not encoded by single neurons in the frequency domain, but rather in the temporal domain across neuronal populations. In fact, the contribution of single olivary neurons to the population activity is actually diminished during movement, because the increase in the size of the active population exceeds the degree to which single neurons increase their firing. That olivary neurons are most likely to fire at the time that the tongue is fully extended may be related to the fact that maximal coordination is required for the tongue to hold a liquid bolus while it retracts into the mouth[13].

It follows that an underlying resonance within the olivary nucleus determines the placement of olivary action potentials during movement. The frequency of the population rhythm during licking is within the frequency range of membrane potential oscillations characteristic of inferior olivary neurons[14,15]. Of relevance is the fact that the membrane potentials of large populations of inferior olivary neurons oscillate synchronously[15] because of extensive electrotonic coupling[16,17]. Subthreshold oscillations in membrane potential, synchronized among populations of olivary neurons, rhythmically modulate olivary excitability[15] and may promote the rhythmic structure of movement[18] by aiding motor-neuronal firing through rhythmic activation of the cerebellum. Our results confirm an initial proposal[19] based on deductions from known function and morphology.

Rhythmic ouput of the inferior olive during movement is punctuated by moments of high synchrony among subsets of

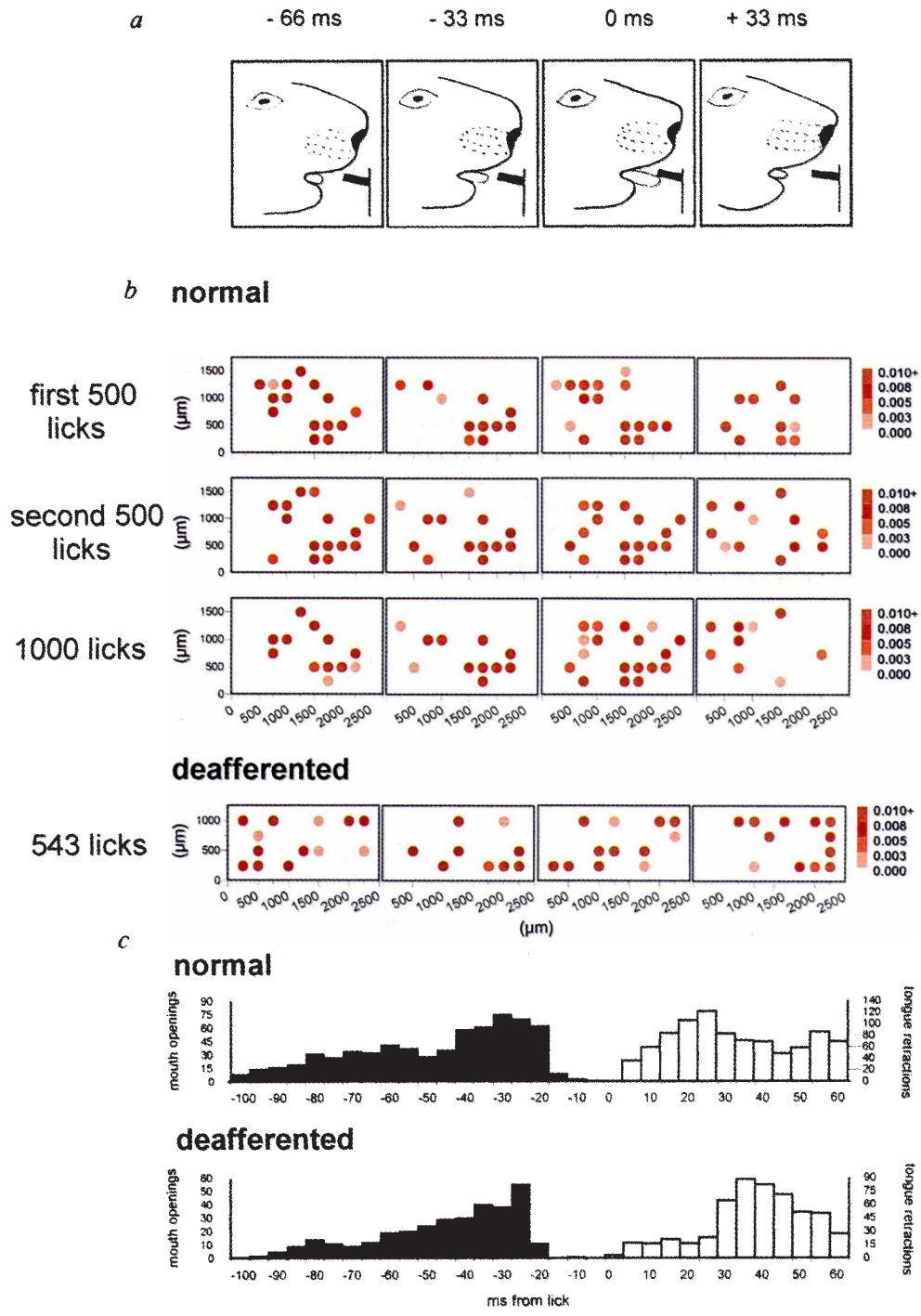

FIG. 4 The spatial distribution of synchronous complex spike firing in a normal and trigeminally deafferented rat during a lick. *a*, Trajectory of the tongue taken from sequential video images of a rat obtained at 30 frames per s. *b*, Spatial plots of synchronously firing Purkinje cells in a matrix of 26 Purkinje cells recorded from the left crus IIa folium of a normal and deafferented rat. Spatial plots of synchronous firing are calculated for 4 epochs of 40 ms and are placed in temporal registration with the overlying video images. For the spatial plots, 0 reflects the postero-lateral limit of the recording matrix. *c*, Histograms of mouth opening (filled bars) and tongue retraction (white bars) relative to 1,000 and 543 licks of the normal and deafferented rats depicted in *b*. Time 0 represents the time that the tongue contacted the target. Bin widths, 5 ms.

olivary neurons. We hypothesize that the axons of synchronously firing Purkinje cells converge upon specific motor zones within the cerebellar nuclei and thereby aid the firing of motor-neuronal pools responsible for executing movement. The cortical region sampled projects to lingual and deglutitional zones within the cerebellar nuclei[20,21]. We propose that the inferior olive is a mosaic of motor representations in which individual muscles are represented by discrete neuronal ensembles embedded within a large electrically coupled network. Dynamic rearrangement of electrotonic coupling within the olivary nucleus, controlled by the deep cerebellar nuclei[22–24], may permit neuronal clusters representing different muscles to be selectively coupled and to fire synchronously when those muscles must be simultaneously engaged during movement. Our results suggest that the inferior olive is an electrically malleable substrate from which unique motor synergies can be sculpted. □

Received 2 September 1994; accepted 3 February 1995.

1. Wilson, W. C. & Magoun, H. W. *J. comp. Neurol.* **83,** 69–77 (1945).
2. Murphy, M. G. & O'Leary, J. L. *Arch. Neurol.* **24,** 145–157 (1971).
3. Eccles, J. C., Llinás, R. & Sasaki, K. *J. Physiol., Lond.* **182,** 268–296 (1966).
4. Desclin, J. C. *Brain Res.* **77,** 365–384 (1974).
5. Sasaki, K., Bower, J. M. & Llinás, R. *Eur. J. Neurosci.* **1,** 572–586 (1989).
6. Llinás, R. & Sasaki, K. *Eur. J. Neurosci.* **1,** 587–602 (1989).
7. Sugihara, I., Lang, E. J. & Llinás, R. *J. Physiol., Lond.* **470,** 243–271 (1993).
8. Keehn, J. D. & Arnold, E. M. M. *Science* **132,** 739–741 (1960).
9. Brooks, V. B. & Thach, W. T. in *Motor Control* Vol. 2 *Handbook of Physiology* 877–946 (American Physiological Society, Maryland, 1981).
10. Box, G. E. P., Jenkins, G. M. & Reinsel, G. C. *Time Series Analysis* 3rd edn (Prentice Hall, New Jersey, 1994).
11. Gerstein, G. L. & Kiang, W. Y. *Biophys. J.* **1,** 15–28 (1960).

12. Winer, B. J. *Statistical Principles in Experimental Design* (McGraw-Hill, New York, 1971).
13. Ziegler, H. P. in *Thirst: Physiological and Psychological Aspects* 241–257 (Springer, New York, 1991).
14. Llinás, R. & Yarom, Y. *J. Physiol., Lond.* **315,** 549–567 (1981).
15. Llinás, R. & Yarom, Y. *J. Physiol., Lond.* **376,** 163–182 (1986).
16. Sotelo, C., Llinás, R. & Baker, R. *J. Neurophysiol.* **37,** 541–559 (1974).
17. King, J. S. *J. comp. Neurol.* **165,** 387–400 (1976).
18. Vallbo, A. B. & Wessberg, J. *J. Physiol., Lond.* **469,** 673–691 (1993).
19. Llinás, R. in *Motor Control: Concepts and Issues* (eds Humphrey, D. R. & Freund, H.-J.) 223–242 (Wiley, New York, 1991).
20. Cicerata, F., Anguat, P., Serapide, M. F., Panto, M. R. & Nicotra, G. *Expl Brain Res.* **89,** 352–362 (1992).
21. Buisseret-Delmas, C. & Angaut, P. *Prog. Neurobiol.* **40,** 63–87 (1993).
22. Lang, E. J., Sugihara, I. & Llinás, R. *Soc. Neurosci. Abstr.* **16,** 894 (1990).
23. Sotelo, C., Gotow, T. & Wassef, M. *J. comp. Neurol.* **252,** 32–50 (1986).
24. De Zeeuw, C. I., Holstege, J. C., Ruigrok, T. J. H. & Voogd, J. *J. comp. Neurol.* **284,** 12–35 (1989).
25. Larsell, O. *The Comparative Anatomy and Histology of the Cerebellum from Monotremes through Apes* (ed. Jansen, J.) (Univ. of Minnesota Press, Minneapolis, 1970).

ACKNOWLEDGEMENTS. We thank P. Reimann for photographic assistance. This research was supported by grants from the United States Public Health Service and the Office of Naval Research.

An essential role for Rac in Ras transformation

Rong-Guo Qiu, Jing Chen, David Kirn, Frank McCormick & Marc Symons

Onyx Pharmaceuticals, 3031 Research Drive, Richmond, California 94806, USA

THE GTPase Rac1 is a key component in the reorganization of the actin cytoskeleton that is induced by growth factors or oncogenic Ras[1]. Here we investigate the role of Rac1 in cell transformation and show that Rat1 fibroblasts expressing activated Val-12 Rac1 (Rac1 with valine at residue 12) display all the hallmarks of malignant transformation. In a focus-forming assay in NIH3T3 fibroblasts to measure the efficiency of transformation, we found that dominant-negative Asn-17 Rac1 inhibited focus formation by oncogenic Ras, but not by RafCAAX, a Raf kinase targeted to the plasma membrane by virtue of the addition of a carboxy-terminal localization signal from K-Ras. This indicates that Rac is essential for transformation by Ras. In addition, Val-12 Rac1 synergizes strongly with RafCAAX in focus-formation assays, indicating that oncogenic Ras drives both the Rac and MAP-kinase pathways, which cooperate to cause transformation.

We have established Rat1 fibroblast lines expressing Val-12 (V12) Rac1 or Asn-17 (N17) Rac1 driven by a tetracycline-repressible promoter[2,3]. V12-Rac1-expressing fibroblasts show a large increase in the number of lamellipodia and a concomitant stimulation of pinocytotic activity over vector controls, consistent with results from microinjection of V12-Rac1 expression plasmids and recombinant proteins in other cell lines (ref. 1 and M.S. *et al.*, unpublished results). Also in agreement with previous observations[1], serum-starved N17-Rac1 transfectants showed strong inhibition of ruffling in response to epidermal growth factor (EGF). A full characterization of the actin cytoskeleton, morphology and motility properties of the V12-Rac1- and N17-Rac1-expressing lines will be described elsewhere.

Cell growth of the V12-Rac1-expressing lines was significantly faster than of N17-Rac1 lines (Fig. 1*a*). V12-Rac1 lines grew to higher saturation density, whereas N17-Rac1-transfected lines grew to lower saturation density compared with vector controls (Fig. 1*b*). These results indicate that constitutive activation of Rac1 in Rat1 fibroblasts causes a partial loss of contact inhibition, whereas inhibition of endogenous Rac function by introduction of dominant-negative Rac1 leads to an increase in contact inhibition. V12-Rac1-expressing lines also had a reduced dependence on serum: in the presence of 10% serum, V12-Rac1 lines grew slightly more slowly than vector lines (Fig. 1*a*), whereas growth rates in 0.5% fetal bovine serum were markedly faster than those of vector controls (Fig. 1*c*).

TABLE 1 Agar colony formation and *in vivo* tumour growth of V12 Rac1-expressing lines

Cell line	Relative expression	Soft agar clonability (%)	Tumour incidence	Tumour volume ±s.e.m. (ml)
Val-12 Rac1 1a	+ +	1.2	6/6	2.4 ± 0.7
2a	+ + +	14.3	6/6	2.6 ± 0.4
3a	+	ND	6/6	0.4 ± 0.1
4a	+	ND	6/6	0.8 ± 0.2
9a	+ +	ND	6/6	1.8 ± 0.3
14a	+ + +	14.2	ND	ND
15a	+	4	ND	ND
Asn-17 Rac1 2a	+ + +	0	ND	ND
10	+ +	0	ND	ND
Val-14 RhoA24	+ + +	0	ND	ND
28	+ + +	0	ND	ND
Vector 5, 6, 8	NA	0	0	0

ND, not determined; NA, not applicable. Rat1 fibroblast lines expressing Myc-tagged V14 RhoA were established following a procedure similar to that used for the Rac1 mutant lines described in Fig. 1 legend. For the soft-agar clonability assays, tetracycline was withdrawn two days before the start of each experiment to induce full expression of mutant Rac1 and RhoA proteins. Cells were plated at a density of 2×10^3 cells per well in 6-well plates sandwiched by 1 ml bottom agar (0.6%) and 1 ml top agar (0.3%). Cells were fed every week by adding a new layer of top agar. After 4 weeks, colonies larger than 75 μm were scored under the microscope. Data are representative of 2 independent experiments. Tumour growth was determined in athymic nude mice following subcutaneous injection of 1×10^7 cells in each flank of 3 mice. Tumour volume was estimated using the following formula: (maximal tumour diameter) × (perpendicular) × (mean of the two measurements).

When tested for the ability to grow in soft agar, V12-Rac1-expressing lines generated colonies within one week with an efficiency that roughly correlated with V12-Rac1 expression (Table 1), indicating that constitutive activation of Rac1 leads to anchorage-independence of growth. Rat1 fibroblasts expressing constitutively active V14 RhoA (ref. 4) did not produce any colonies in soft agar (Table 1). V12-Rac1-expressing lines were also tested for their ability to induce tumours *in vivo* by subcutaneous inoculation into athymic nude mice. All the V12-Rac1-transfected lines studied induced palpable tumours within two weeks, which grew progressively. Tumour-growth rate correlated well with V12-Rac1 expression. No tumours were formed during a period of two months in mice inoculated with the same number of vector control fibroblasts (Table 1). Thus, V12-Rac1-expressing lines display all the features of transformed cells.

Stimulation of lamellipodial outgrowth by oncogenic Ras depends on Rac (ref. 1). To test whether Rac1 is also important for Ras-induced transformation, focus-formation was assayed in NIH3T3 cells using V12-H-Ras in the presence or absence of cotransfected N17-Rac1 or dominant negative Ala-218/Ala-222 MEK1 (ref. 5). As expected, A218/A222 MEK1 inhibited Ras-induced focus formation in a dose-dependent manner (Fig. 2*a*). N17 Rac1 inhibited Ras-induced focus formation with a dose-dependence like A218/A222 MEK1, indicating that Rac is necessary for Ras transformation. In contrast, N17 Rac1 did not inhibit focus formation by RafCAAX, which constitutively activates the MAP-kinase pathway[6,7] (Fig. 2*b*). These and earlier observations, that N17 Rac1 inhibits reorganization of the actin cytoskeleton induced by injection of oncogenic Ras, strongly suggest that Rac acts downstream of Ras and drives a signalling cascade that parallels the MAP kinase pathway. We therefore tested for synergism between these two pathways using focus-formation assays. Co-transfection of V12 Rac1 with RafCAAX, at plasmid concentrations that produce few foci when transfected individually, caused a remarkable increase in transforming activity (Fig. 3), indicating a high degree of cooperativity between the Rac and MAP-kinase pathways.